Ultra-High Repetition Rate Absorption Spectroscopy with Low Noise Supercontinuum Radiation generated in an All-Normal Dispersion Fibre

S. Dupont,[1] Z. Qu,[2] S.-S. Kiwanuka,[2] L. E. Hooper,[3] J. C. Knight,[3] S. R. Keiding,[1] and C. F. Kaminski[2, a)]
[1)] *Department of Chemistry, Aarhus University, DK-8000 Aarhus C, Denmark*
[2)] *Department of Chemical Engineering and Biotechnology, University of Cambridge, Pembroke Street, Cambridge CB2 3RA, U.K.*
[3)] *Centre for Photonics and Photonic Materials, Department of Physics, University of Bath, Bath, BA2 7AY, UK*

We report use of a dispersed supercontinuum generated in an all-normal-dispersion fibre to record low-noise spectra from atmospheric molecules at least an order of magnitude faster than has been previously reported. Supercontinuum generation in standard, anomalous dispersion photonic-crystal fibres is inherently connected with large pulse-to-pulse fluctuations resulting in detrimental consequences for high resolution spectroscopy if temporal averaging is not permitted. Replacing the standard PCF with a specially designed all-normal dispersion PCF we find that a substantially superior noise performance is achieved and present its use for high repetition rate absorption spectroscopy where spectra covering 100s of nm in spectral bandwidth can be captured of gases at 100s of kHz repetition rates.

INTRODUCTION

Over the last two decades supercontinuum (SC) light sources have become key enablers in several branches of optical physics. The advent of the photonic-crystal fibre (PCF) and wide availability of short pulse pump laser sources mean that SC generation is now a routine operation to motor numerous research applications in diverse fields. PCF generated SC has revolutionised the ability to generate optical frequency combs[1,2] and has enabled broadband cavity ring-down spectroscopy[3]. Sophisticated molecular spectroscopy techniques such as CARS[4] and optical coherence tomography[5,6] have likewise benefited from these sources. The combined intensity and spectral range of supercontinuum radiation is superior compared to other light sources, and this is the reason for its versatile use. In recent years, SC has been extended into the mid IR, making it even more useful for spectroscopy, as fundamental absorption bands can be targeted directly[7,8].

The broad bandwidth afforded by SC radiation is particularly useful for broadband spectroscopy applications, for example to identify species composition and concentration in gaseous or liquid mixtures[6,9–11]. For many applications a high temporal resolution is desirable for example to probe reacting flows, in energy conversion and in industrial applications, where phenomena occur on ms or even shorter timescales. SC radiation offers enormous potential in these latter applications because of its inherent bandwidth and short pulse nature.

One method to utilise SC sources for high-speed spectroscopy is to pass the broad bandwidth light pulses through a highly dispersive fibre: Group velocity dispersion then causes different colours to exit at different times which results in a wavelength-to-time conversion of the output light. Spectra can then be measured in the time domain via a fast photo detector and a transient digitizer. Effectively, one is thus able to generate an ultra-rapid wavelength sweep of a broad bandwidth light source[12,13].

Previously, this has been used to investigate the noise characteristics of SC sources[14,15]. We have made use of the this principle to pioneer the development of ultra-high repetition rate absorption spectroscopy of gaseous substances[16,17]. In previous applications we used SC generated in fibres pumped in the anomalous dispersion regime using ps laser sources. This allows for very broad bandwidth supercontinua to be generated but associated noise characteristics caused large shot-to-shot instability and this made it necessary to average spectra over many subsequent laser pulses, limiting the speed which spectra could be recorded.

The purpose here is to investigate the performance of SC generated in an all-normal PCF which was specially designed to lead to better noise performance from shot to shot[18]. We show that significantly better stability is achievable in these fibres from shot to shot, even in the long pump pulse regime. Finally we demonstrate the superior performance for ultra-high repetition rate absorption spectroscopy. The lower noise reduces the requirement for pulse averaging of spectra and we demonstrate speed improvements of at least a factor of 10 over previous implementations, permitting entire rovibrational spectra to be captured at over 100 kHz repetition rates. This permits ultra-high bandwidth absorption spectroscopy in dynamic environments.

[a)] Corresponding author: cfk23@cam.ac.uk

BACKGROUND

For efficient broad bandwidth supercontinuum generation PCFs are usually pumped in the anomalous dispersion regime, close to their zero dispersion wavelength. This leads to the generation of solitons and dispersive wave trapping, facilitating the generation of broad bandwidth spectra[19–21]. In the long pulse regime ($\geq$ ps) however, the ensuing soliton dynamics are governed by noise-seeded modulation instabilities, leading to soliton fission and substantial pulse-to-pulse fluctuations[19,22,23]. This is the reason why temporal averaging over many pulses is usually requirede when SC sources are used in various applications[9]. For this reason we designed a fibre with a dispersion profile that is optimised for noise-free supercontinuum generation. The fibre has a flat, all normal dispersion profile around the zero dispersion wavelength and we avoid soliton generation. Spectral broadening is thus primarily achieved via self-phase modulation[24]. We characterize the pulse-to-pulse characteristics of the generated supercontinua in comparison with those obtained in standard PCF and then demonstrate the performance improvement for rapid wavelength sweeping spectroscopy of gaseous absorbers[18].

The cross section and measured dispersion profile of the all-normal dispersion PCF is displayed in Figure 1, left hand panel[18]. The dispersion is negative (normal) over the entire range from 700 nm to 1500 nm enabling soliton free SC generation at the pump wavelength (1060 nm). The flatness of the profile around the pump wavelength reduces third-order dispersion. The right hand panel of Figure 1 shows the dispersion profile of the standard, anomalous, PCF used here where the zero-dispersion wavelength is tailored towards shorter wavelengths. Above 1040 nm, the dispersion D is positive (anomalous). Pumping at 1060 nm thus produces solitons which produces broader but also noisier SC spectra than is the case for the former.

EXPERIMENTAL SETUP

The SC output from the two fibres was investigated using the technique described in ref. 12–16. The setup is shown schematically in Figure 2. Supercontinuum was generated in either the all-normal dispersion fibre (ND) or in the anomalous dispersion (AD) fibre shown in Figure 1. The pump source was an ytterbium-doped fibre laser operating at 1060 nm. The input pulse length is 5 ps with maximal pulse energy of 1.0 µJ produced at a repetition rate of 700 kHz. A time-of-flight technique is used to characterise the spectrum of a single SC pulse[13]. The SC pulse is stretched from picoseconds to 100s of nanoseconds upon passage through a dispersion-compensating module (DCM), featuring a dispersion which varies from 0.9 ns/nm at 1300 nm to 1.5 ns/nm at 1500 nm (Fujikura, G652-C+L-band SC-DCFM). The stretched pulses were subsequently recorded using a photodiode with 14 GHz bandwidth in combination with an 8 GHz real time sampling oscilloscope (Tektronix - TDS6804B). Using the known dispersion characteristics of the DCM allowed transformation of the recorded signal time trace back to the wavelength domain. The sampling bandwidth translates into a spectral resolution of approximately 0.2 nm in the wavelength range from 1250 nm to 1550 nm at sweep rates of 0.6 nm/ns.

NOISE PERFORMANCE

Figure 3 shows a comparison of single-shot supercontinuum pulses generated in the all-normal dispersion fibre (ND) (top left panel) and in the anomalous dispersion fibre (AD) (top right panel). Blue traces represent data at the sampling resolution. The red/white curves are the long-time averages of the data. For the AD fibre (top right panel), the green/white superimposed traces represent the data with a low pass filter applied, which was done to remove high frequency noise. The two different analyses facilitate a comparison of the shot-to-shot variation in noise behaviour between the two fibre outputs. Both fibres show high frequency noise, but in addition the AD fibre also exhibits significant shot-to-shot variations in the pulse envelope due to soliton dynamics[15,22,25,26]. Especially at wavelengths above 1400 nm, the fluctuations are noteworthy. These are absent in the ND fibre as it does not support solitons, and the envelope of single pulses coincides better with the long-time average. The red/white curve plotted over the bottom spectrum for the AD fibre is the long-term average, which exposes the lack of resemblance of individual spectra from their mean due to the higher fluctuations arising from soliton dynamics.

The two lower panels in Figure 3 show spectra of 200 consecutive pulses which are stacked along the y-axis, to illustrate the pulse-to-pulse fluctuations[15]. Clearly again much larger fluctuations are seen at longer wavelengths for the anomalous dispersion fibre compared to the all-normal fibre. The intensity dip around 1375 nm for both fibres is due to intrinsic absorption in the dispersion-compensating module used for stretching the supercontinuum. This absorption appears to be broader for the AD fibre than for the ND fibre, but this is as a result of the more fluctuating nature of corresponding single-pulse spectra in the former case.

A more quantitative investigation of the wavelength dependent supercontinuum noise was performed by analysing the higher-order moments (coefficient of variation, skewness and kurtosis), as suggested in ref. 27. The coefficient of variation C_v is defined as the standard deviation divided by the mean and is therefore inversely proportional to the signal-to-noise ratio. The skewness γ is a measure of the asymmetry of the distribution and a high kurtosis κ is an expression of long tails. A Gaussian distribution has both zero skewness and kurtosis. The three lower panels in Figure 4 show the higher-order

moments for both the ND fibre (blue) and the AD fibre (red). The analysis is done for the entire wavelength range at a sampling resolution of 0.2 nm. In general a better performance is seen for the ND fibre. The lower coefficient of variation of the ND fibre results in a higher signal-to-noise ratio and will improve the performance in applications where averaging is normally needed. As expected a higher skewness and kurtosis is seen for the AD fibre. This is due to the Raman-shifting solitons depending on input-pulse noise, which had been investigated earlier in the context of rogue waves[28], and also experimentally[14].

To quantify the performance of the fibres when used in absorption spectroscopy we introduce here a noise parameter for which we calculate the absolute difference between a mean of n single spectra, $\lambda_{\langle n\rangle}$, and a spectrum averaged over 10,000 shots, $\lambda_{\langle 10{,}000\rangle}$. The difference is then summed over all wavelengths and normalised to the total signal in the average spectrum. We thus define the noise parameter $N_{\langle n\rangle}$ for the mean of n pulses as:

$$N_{\langle n\rangle} = \frac{\sum_{\lambda} |\lambda_{\langle n\rangle} - \lambda_{\langle 10{,}000\rangle}|}{\sum_{\lambda} \lambda_{\langle 10{,}000\rangle}}. \quad (1)$$

Figure 4 shows $N_{\langle n\rangle}$ for n varying from 1 to 100. Each data point on the plot represents the average of $N_{\langle n\rangle}$ obtained for 100 subsets n. Error bars shown correspond to the standard deviation of $N_{\langle n\rangle}$ from the mean of these 100 subsets. The red trace represents data from the AD fibre, blue represents the ND fibre. It is seen that the traces converge for increasing n, however, the noise parameter is always lower for the ND fibre due to the lack of soliton dynamics exhibited by this fibre. Furthermore, the standard deviation for each data point is consistently much smaller for the ND case, reflecting the higher self-similarity of individual spectra produced in this fibre from shot to shot.

PERFORMANCE IN RAPID WAVELENGTH SWEEPING ABSORPTION SPECTROSCOPY

The analysis in the last section suggests that there should be signicant performance differences between the ND and AD fibre produced supercontinua when used in rapid-sweeping broad-bandwidth absorption spectroscopy. We demonstrate this in practice through measurements of gaseous H_2O in the ambient atmosphere. Figure 5 clearly brings the differences to light. The figure shows measured (blue) and simulated (red) absorption spectra of H_2O for different pulse averaging times. The spectra were obtained by passing the temporally stretched output from the DCM through 3 m of ambient air before collection on the photodiode and transient digitization. In this way an absorption spectrum covering the entire wavelength range from 1250 nm to 1550 nm is swept in less than a microsecond at a spectral resolution of 0.2 nm, corresponding to 8000 spectral data points. For clarity, we present only a small fragment of the full spectral range in Figure 5. A complete spectrum is seen in Figure 6 (right panel). We obtained a reference spectrum by fitting a smooth baseline to the data averaged over 10,000 shots, as seen in the left hand panel of Figure 6. This removes the high frequency water absorptions from the spectrum and the obtained baseline is used for normalisation to plot the H_2O spectra in terms of absorbance units. The top row in Figure 5 shows spectra obtained using the AD fibre for supercontinuum generation, the corresponding case for the ND fibre is shown in the bottom row. The averaging time from left to right is 10 µs (7 pulses), 100 µs (70 pulses) and 14.3 ms (10,000 pulses). The red line corresponds to a HITRAN[29] simulation of the same spectral portion of H_2O over 3 m of air under prevailing experimental conditions. The line positions were convolved with Gaussian line shape functions using a spectral resolution of 0.2 nm, to match the resolution of the experimental setup.

Clearly, simulated and measured spectra are in excellent agreement for both the AD and ND supercontinua for the longest averaging time (14.3 ms). However, as the averaging time is reduced, the two methods diverge dramatically in quality. For the AD spectra soliton noise rapidly degrades the quality of the absorption spectra. Already at 100 µs of averaging, the AD spectrum is clearly compromised by noise, whereas the ND spectrum is hardly affected and agreement with the model remains excellent. For 10 µs averaging, the water spectrum is lost in noise for the AD generated supercontinuum, whilst the ND generated SC still produces perfectly recognisable absorption features in the water spectrum that are easily modeled using HITRAN. It is important to remember that the absorption spectrum covers the entire spectral range from 1250 nm to 1550 nm and an example spectrum covering this rage is shown in Figure 6. The truncation to a 5 nm spectral range is only done in order to emphasise the convincing resemblance with the HITRAN spectrum. The absorption spectra show similar tendencies as seen in the top panel of Figure 4, i.e. a faster convergence and significantly lower fluctuations for the ND fibre compared to the AD fibre. This again underlines the previous observations, that the higher self-similarity of the SC spectra makes the ND fibre much more suitable for broad-bandwidth rapid wavelength sweeping spectroscopy method compared to the more noisy AD fibre. These characteristics will not only be beneficial for the rapid sweeping technique, but are relevant for many other areas, where practical high power SC radiation is used for high speed applications. As the spectral averaging time can be reduced, measurements can either be performed faster or with higher precision. The present data demonstrates that good quality absorption spectroscopy covering 100s of nm in width can be performed at repetition rates exceeding 100 kHz. This opens the door to applications in energy conversion processes e.g. in gas turbines or engines, or for the study of

rapid chemical processes in science or industry.

REFERENCES

[1]Diddams, S. A. *et al.* Direct link between microwave and optical frequencies with a 300 THz femtosecond laser comb. *Phys. Rev. Lett.* **84**, 5102–5105 (2000).

[2]Udem, T., Holzwarth, R. & Hansch, T. Optical frequency metrology. *Nature* **416**, 233–237 (2002).

[3]Thorpe, M. J., Moll, K. D., Jones, R. J., Safdi, B. & Ye, J. Broadband cavity ringdown spectroscopy for sensitive and rapid molecular detection. *Science* **311**, 1595–1599 (2006).

[4]Paulsen, H. N., Hillingsø, K. M., Thøgersen, J., Keiding, S. R. & Larsen, J. J. Coherent anti-stokes raman scattering microscopy with a photonic crystal fiber based light source. *Optics Letters* **28**, 1123–1125 (2003).

[5]Marks, D., Oldenburg, A., Reynolds, J. & Boppart, S. Study of an ultrahigh-numerical-aperture fiber continuum generation source for optical coherence tomography. *Optics Letters* **27**, 2010–2012 (2002).

[6]Moon, S. & Kim, D. Y. Ultra-high-speed optical coherence tomography with a stretched pulse supercontinuum source. *Optics Express* **14**, 11575–11584 (2006).

[7]Xia, C. *et al.* Mid-infrared supercontinuum generation to 4.5 μm in ZBLAN fluoride fibers by nanosecond diode pumping. *Opt. Lett.* **31**, 2553–2555 (2006).

[8]Agger, C. *et al.* ZBLAN supercontinuum generation – detailed comparison between measurement and simulation. *J. Opt. Soc. Am. B* **29**, 635–645 (2012).

[9]Kaminski, C. F., Watt, R. S., Elder, A. D., Frank, J. H. & Hult, J. Supercontinuum radiation for applications in chemical sensing and microscopy. *App. Phys. B* **92**, 367 (2008).

[10]Kano, H. & Hamaguchi, H. Ultrabroadband (> 2500 cm^{-1}) multiplex coherent anti-Stokes Raman scattering microspectroscopy using a supercontinuum generated from a photonic crystal fiber. *Applied Physics Letters* **86** (2005).

[11]Langridge, J. M. *et al.* Cavity enhanced absorption spectroscopy of multiple trace gas species using a supercontinuum radiation source. *Optics Express* **16**, 10178–10188 (2008).

[12]Kelkar, P., Coppinger, F., Bhushan, A. & Jalali, B. Time-domain optical sensing. *Electronics Letters* **35**, 1661–1662 (1999).

[13]Hult, J., Watt, R. S. & Kaminski, C. F. Dispersion measurement in optical fibers using supercontinuum pulses. *Journal of Lightwave Technology* **25**, 820–824 (2007).

[14]Solli, D. R., Ropers, C., Koonath, P. & Jalali, B. Optical rogue waves. *Nature* **450**, 1054–U7 (2007).

[15]Wetzel, B. *et al.* Real-time full bandwidth measurement of spectral noise in supercontinuum generation. *Scientific Reports* **2** (2012).

[16]Hult, J., Watt, R. & Kaminski, C. F. High bandwidth absorption spectroscopy with a dispersed supercontinuum source. *Optics Express* **15**, 11385–11395 (2007).

[17]Watt, R. S., Kaminski, C. F. & Hult, J. Generation of supercontinuum radiation in conventional single-mode fibre and its application to broadband absorption spectroscopy. *App. Phys. B* **90**, 47–53 (2008).

[18]Hooper, L., Mosley, P. J., Muir, A. C., Wadsworth, W. J. & Knight, J. C. Coherent supercontinuum generation in photonic crystal fiber with all-normal group velocity dispersion. *Optics Express* **19**, 4902–4907 (2011).

[19]Dudley, J. M. & Coen, S. Coherence properties of supercontinuum spectra generated in photonic crystal and tapered optical fibers. *Opt. Lett.* **27**, 1080–1082 (2002).

[20]Dudley, J. M., Genty, G. & Coen, S. Supercontinuum generation in photonic crystal fiber. *Reviews of Modern Physics* **78**, 1135–1184 (2006).

[21]Russell, P. S. J. Photonic-crystal fibers. *J. Lightwave Technol.* **24**, 4729–4749 (2006).

[22]Gu, A. *et al.* Experimental studies of the coherence of microstructure-fiber supercontinuum. *Optics Express* **11**, 297–2703 (2003).

[23]Liu, C., Rees, E. J., Laurila, T., Jian, S. & Kaminski, C. F. Periodic interactions between solitons and dispersive waves during the generation of non-coherent supercontinuum radiation. *Optics Express* **20**, 6316–6324 (2012).

[24]Heidt, A. M. *et al.* Coherent octave spanning near-infrared and visible supercontinuum generation in all-normal dispersion photonic crystal fibers. *Optics Express* **19**, 3775–3787 (2011).

[25]Corwin, K. L. *et al.* Fundamental noise limitations to supercontinuum generation in microstructure fiber. *Phys. Rev. Lett.* **90**, 113904 (2003).

[26]Liu, C., Rees, E. J., Laurila, T., Jian, S. & Kaminski, C. F. Predicting supercontinuum pulse collisions with simulations exhibiting temporal aliasing. *Optics Letters* **35**, 4145–4147 (2010).

[27]Sørensen, S. T., Bang, O., Wetzel, B. & Dudley, J. M. Describing supercontinuum noise and rogue wave statistics using higher-order moments. *Optics Communications* **285**, 2451–2455 (2012).

[28]Liu, C., Rees, E. J., Laurila, T., Jian, S. & Kaminski, C. F. An adaptive filter for studying the life cycle of optical rogue waves. *Optics Express* **18**, 26113–26122 (2010).

[29]Rothman, L. *et al.* The HITRAN 2004 molecular spectroscopic database. *Journal of quantitative spectroscopy & radiative transfer* **96**, 139–204 (2005).

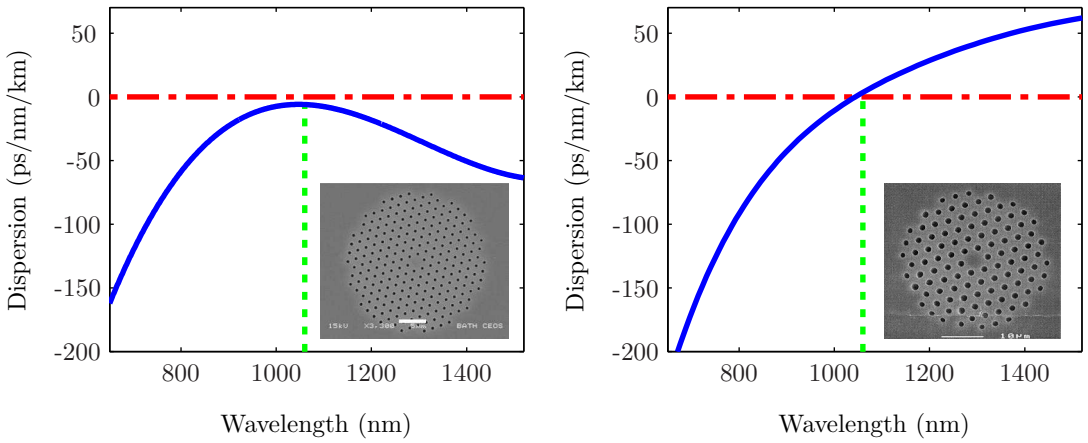

FIG. 1. Measured dispersion profiles-, of the all-normal dispersion PCF (left panel) produced for low noise wavelength sweep spectroscopy and a anomalous PCF (right panel). Insets show scanning electron microscope micrographs of fibre cross-sections. Scale bars are 5 µm and 10 µm, respectively. The red lines indicate the zero dispersion wavelength, green lines correspond to the pump wavelength at 1060 nm.

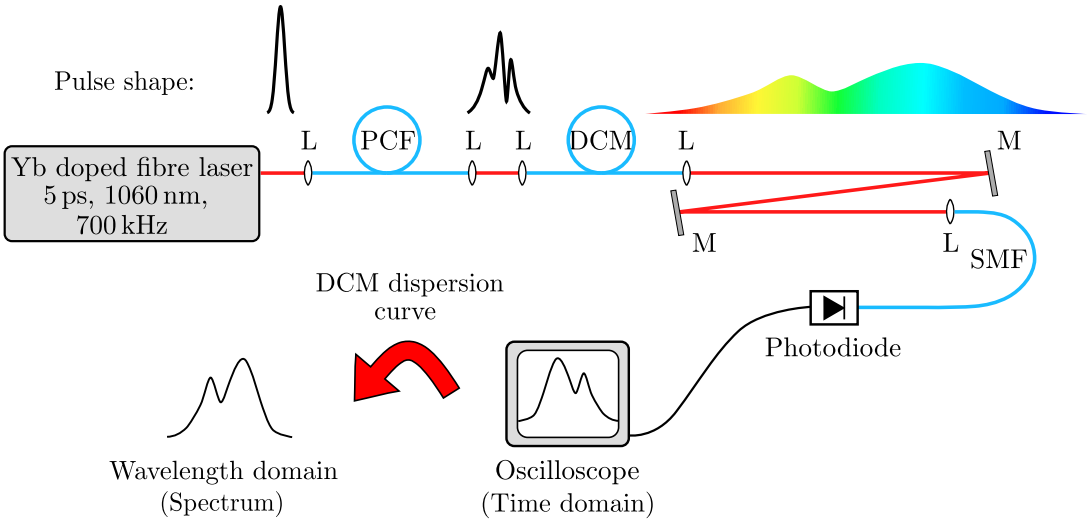

FIG. 2. Experimental setup. A short (∼ ps) pulse from the pump laser generates a supercontinuum in the PCF which is subsequently stretched to nearly 1 µs in the DCM. The resulting wavelength sweep is captured with a fast photodiode and transiently digitized. Using the known dispersion characteristics of the DCM the spectrum of the pulse can be recovered. SMF = Single mode fibre, L = Lens, M = Mirror.

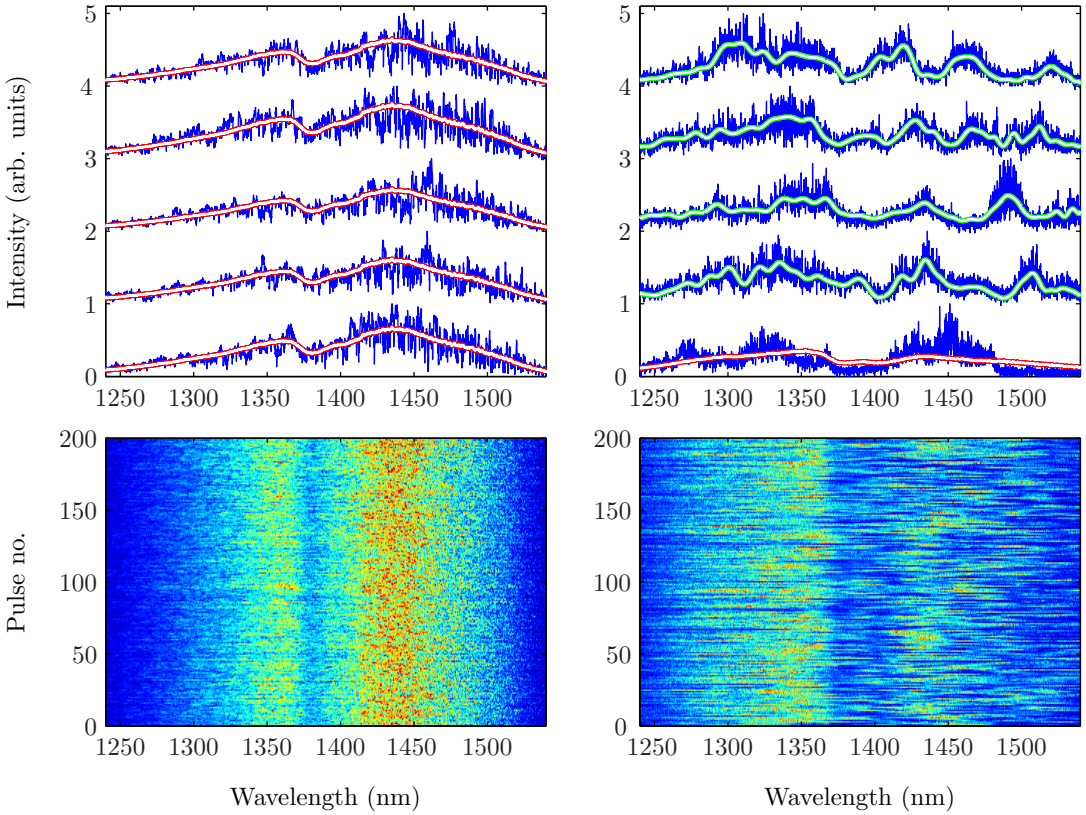

FIG. 3. Single shot spectra from the all-normal PCF (left panels) and the anomalous PCF (right panels). Top Left: The red/white line represents a long term average (10,000 shots) of the all normal spectrum. It can be seen that each individual trace mimics the shape of the average spectrum well. Top Right: The green/white lines shows a low pass filtered version of each individual (blue) trace. The red/white line in the lowest spectrum shows the long term average of the anomalous supercontinua produced. As can be seen, the shot-to-shot variation of individual sectra deviates very significantly from the long term average, in stark contrast to the all normal SC shown to the left. Bottom: 200 consecutive single pulse spectra plotted using a colour map in which red denotes high intensity and blue denotes low intensity. Left is the all-normal fibre and right is the anomalous fibre.

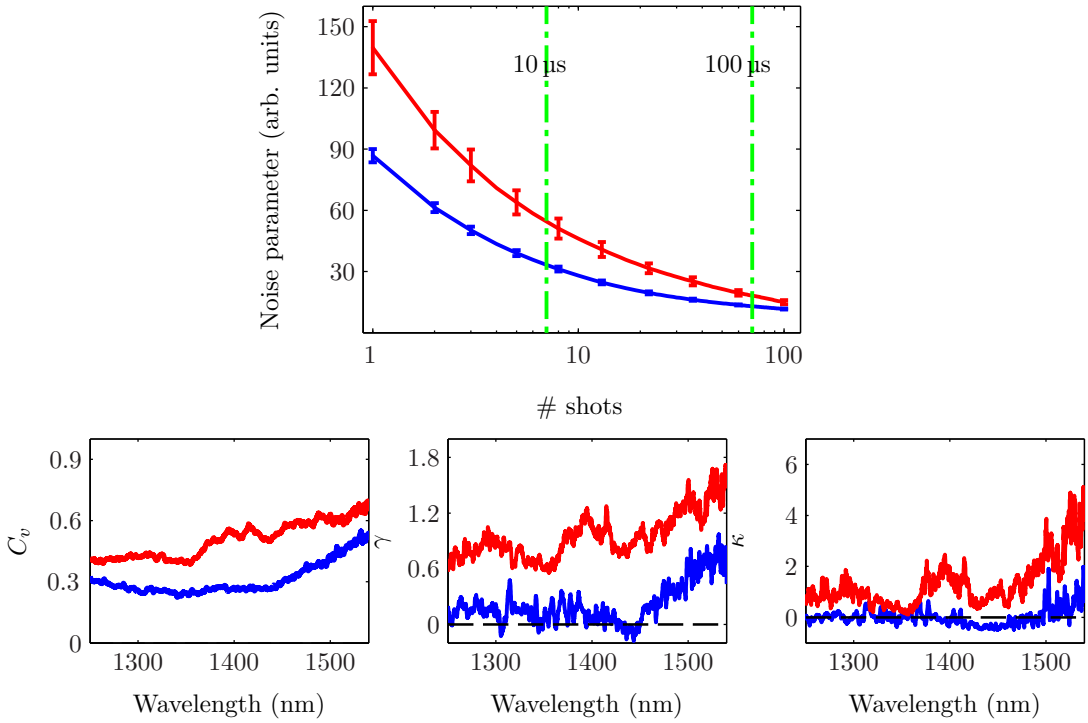

FIG. 4. Noise performance analysis. Top panel shows the noise parameter (see text) calculated for the output spectrum of the AD fibre (red curve) and ND fibre (blue curve). The two vertical green lines correspond to 10 µs and 100 µs averaging. Bottom: Graphs showing coefficient of variation C_v, skewness γ and kurtosis κ, respectively. Red curves correspond to AD fibre and blue to ND fibre.

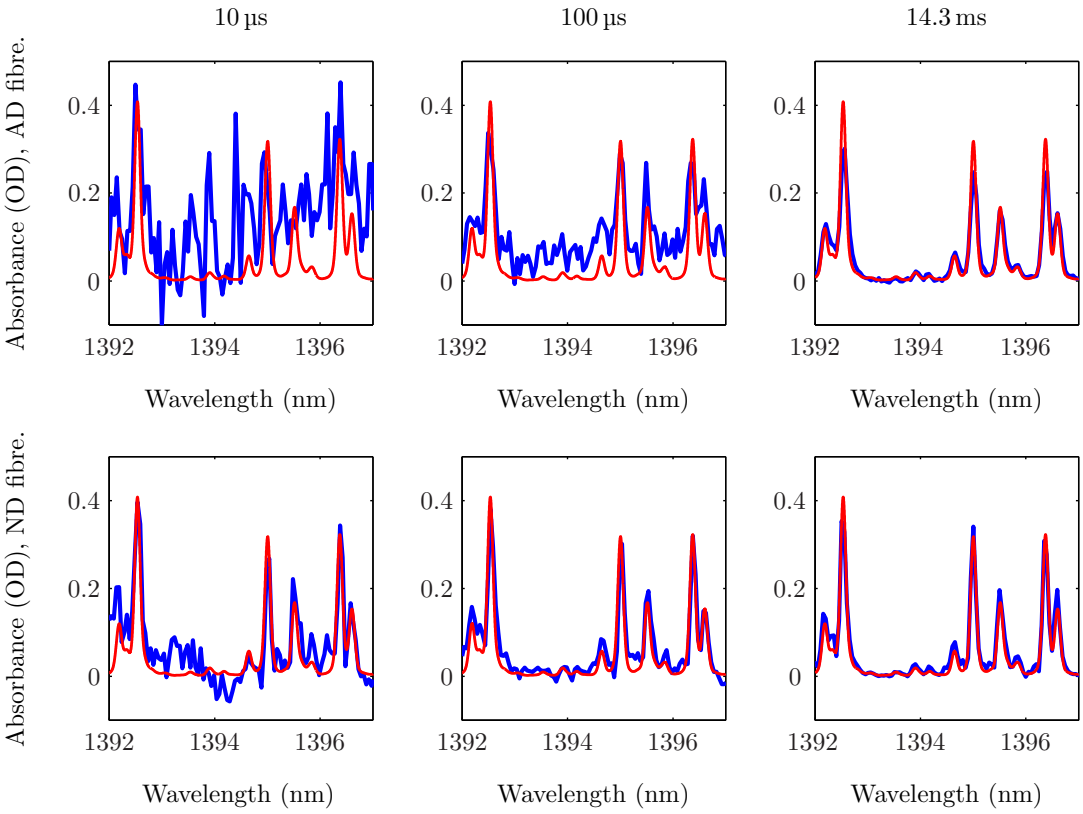

FIG. 5. Absorption measurements of 3 m of ambient air. Top row is the AD fibre, bottom is the ND fibre. Averaging time is 10 µs, 100 µs and 14.3 ms from left to right. The superimposed red line is the absorption spectrum of H_2O based on the HITRAN database. The spectra cover the entire wavelength range from 1250 nm to 1550 nm; truncation is done for clarity.

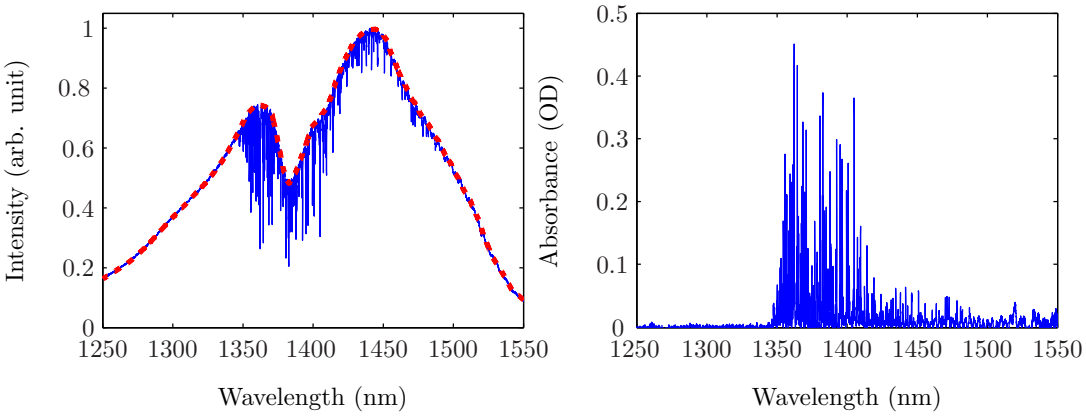

FIG. 6. Average spectrum of 10,000 shots after passage through 3 m of ambient air. The red curve in the left hand panel is the baseline fit used to calculate the absorbance shown in the right hand panel. This gives the full H_2O absorption spectrum covering the entire wavelength range from 1250 nm to 1550 nm. The absorption spectra in Figure 5 are zooms of spectra like this.